***Highlights**

Highlights:

- The molecular orientation within non-crystalline transport materials can be controlled.
- This affects the charge-injection efficiency at organic-organic interfaces, where
- The energy-level alignment is determined by the intramolecular polar bond orientation.

*Graphical Abstract

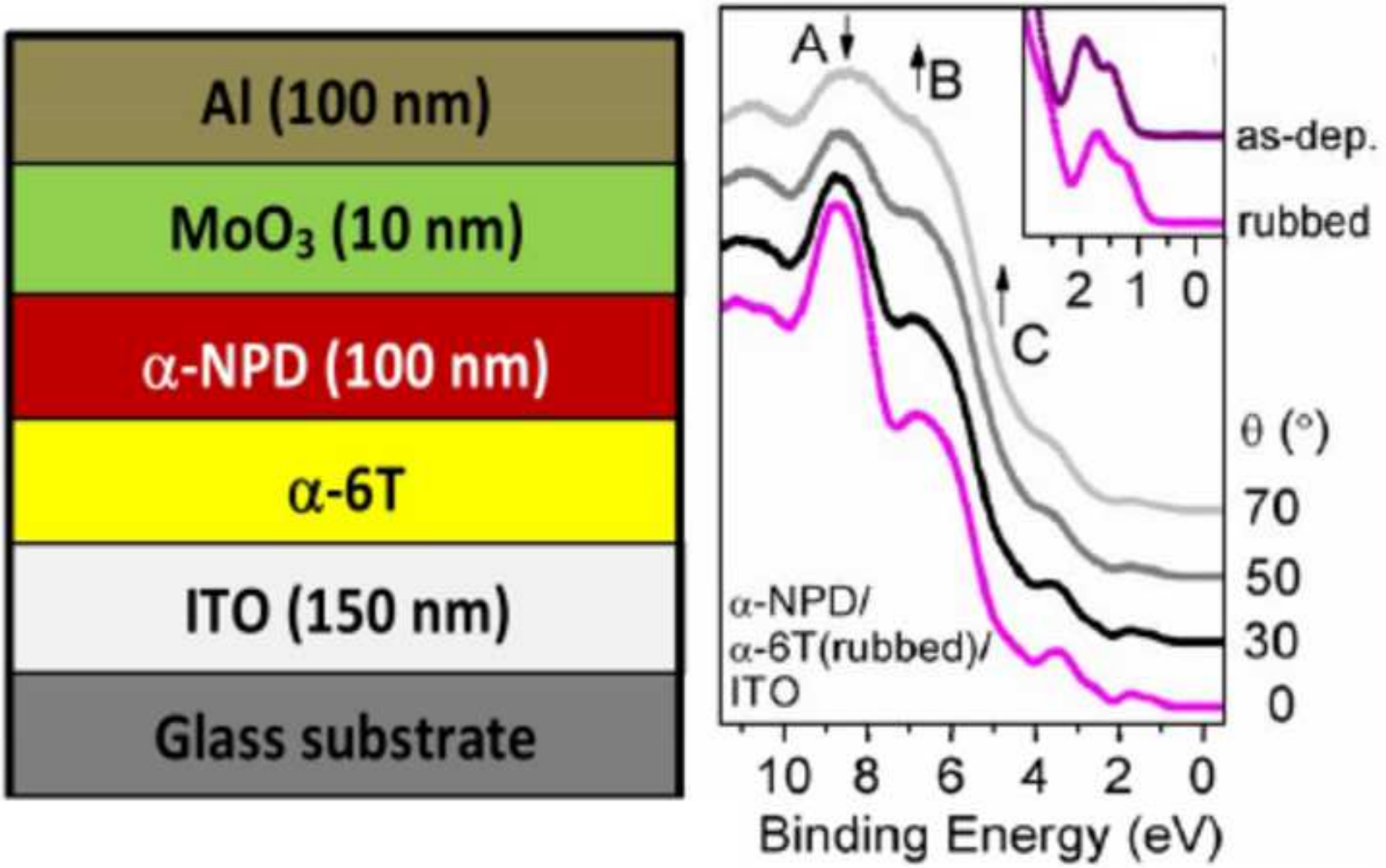

Molecular order, charge injection efficiency and the role of intramolecular polar bonds at organic/organic heterointerfaces

Y. Wang*, T. Matsushima, H. Murata, A. Fleurence, Y. Yamada-Takamura, and R. Friedlein*

School of Materials Science, Japan Advanced Institute of Science and Technology, 1-1 Asahidai, Nomi, Ishikawa 923-1292, Japan

ABSTRACT

The effect of orientational changes in thin films of the non-crystalline hole transport material α–*N*–*N*′–diphenyl *N*–*N*′*'*–bis(1 naphthayl)–*1*,*1*′–biphenyl–*4*,*4*′–diamine (α–NPD) on the energy level alignment and the film electronic structure has been investigated by angle-resolved ultraviolet photoelectron spectroscopy and related to the transport characteristics of hole-only devices. Changes in the anisotropic α-sexithiophene (α–6T) substrate from a "standing" to a "flat" molecular orientation induced by mechanical rubbing lead to molecular order and a preferential orientation in subsequently deposited thin α–NPD films and cause a reduction of the charge injection barrier at the organic/organic interface. The results show that the height of this barrier is determined by the surface dipoles of the individual organic films that relate to the orientation of intramolecular polar bonds at the interface.

*Corresponding authors. Address: School of Materials Science, Japan Advanced Institute of Science and Technology, 1-1 Asahidai, Nomi, Ishikawa 923-1292, Japan (Y. Wang and R. Friedlein)

E-mail address: wang-y@jaist.ac.jp (Y. Wang), friedl@jaist.ac.jp (R. Friedlein)

Keywords: Organic-organic interface

Charge-injection barrier

α-NPD

Ultraviolet photoelectron spectroscopy

1. Introduction

While over the last decades, the mechanisms underlying the functioning of organic electronics devices have been the topic of intense research such that in particular organic light-emitting devices (OLEDs) do now rapidly mature into new applications and products [1-3]. In such OLEDs, amorphous or non-crystalline materials are commonly employed. It has been found that these amorphous films may exhibit a preferential orientation[4] or even a particular defined local packing. This affects charge carrier transport and light emission that depend strongly on the local moleculer order [5-10]. In a comprehensive study, Adachi and coworkers investigated the molecular orientation and electronic properties of a large number of organic amorphous thin film materials and found that linear or planar molecules show a tendency to orient flat with respect to the substrates [4]. Longer molecules are inclined to form films with a larger anisotropy [4]. It was also shown that the molecular orientation of linear-shaped 4,4'-bis[(*N*-carbazole)styryl]biphenyl molecules can be controlled by the substrate roughness and temperature [11]. Charge carrier mobilities have been observed to be higher for films with a horizontal molecular orientation as compared to others highlighting the significant role of the molecular orientation on the charge-transport characteristics of organic amorphous films. Introducing highly oriented *p*-sexiphenyl (6P) films as the emissive layer of light-emitting devices, Era *et al.* demonstrated polarized electroluminescence from oriented 6P films [7]. Yanagi *et al.* prepared 6P films exhibiting either a "lying" and or a "standing" orientation, denoted *l*- and *s*-6P, epitaxially on KCl (001) surfaces and constructed a multilayered electroluminescent device containing these 6P films using indium tin oxide

(ITO) as electrode material and 2-(4-biphenylyl)-5-(4-tertbutylphenyl)-1,3,4-oxadiazole (PBD) as the electron transport layer [9]. As compared to the *s*-6P devices, those employing an *l*-6P layer emitted a higher electroluminescence (EL) intensity within a narrower spectrum, even at a lower driving voltage. These examples demonstrate that optimizing the molecular packing and orientation in active layers is an efficient way to control the charge transport and optical properties in order to further enhance the performance of OLEDs.

As shown by Arai *et al.*, amorphous but simultaneously uniaxially and horizontally oriented organic films can be obtained by mechanical brushing [12]. When used in OLEDs with polarized emission, the EL intensity was higher parallel to the brushing direction as compared to the perpendicular one. Nevertheless, simple and practical methods for the effective control of the molecular orientation and of the resulting electronic properties are still limited. In this context, recently, we reported that upon mechanical rubbing of thin α–sexithiophene (α–6T, the chemical structure shown in Fig. 1a) films on ITO substrates, using a Nylon cloth, the molecular orientation changes from the "standing" to a "lying" configuration [13]. Using the "flat" α-6T films as substrates for α–NPD (see chemical structure in Fig. 1a) films in hole-only devices, current densities are dramatically increased (42 times at a driving voltage of 1.0 V) with respect to devices with a "lying" α–6T film.

In the present work, angle-dependent ultraviolet photoelectron spectroscopy (UPS) has been used to investigate the molecular orientation and electronic structure of the α–6T and subsequently deposited α-NPD films providing infomation on the energy level alignment in the devices. The mechanism responsible for the enhanced hole injection at the organic/organic interface is clarified and linked to changes in the preferential molecular orientation within the α–NPD films caused by the rubbing of the α–6T substrate.

2. Experimental and calculations

ITO substrates have been cleaned by conventional ultra-sonication and ultraviolet-ozone treatment [13]. α–6T (Aldrich) films with a thickness of about 15 nm were then deposited under high-vacuum conditions (of 2.0×10^{-7} mbar) onto the cleaned ITO substrates, at the rate of about 1 Å/s. Some of the sample surfaces have been rubbed 15 times with a dust-free Nylon cloth inside a nitrogen-filled glove box. For the samples prepared for the UPS measurements, α-NPD (Nippon Steel Chemical) films with a thickness of about 10 nm have then been deposited under ultra-high vacuum conditions onto either the as-deposited or rubbed α–6T films. The particular thickness has been chosen in order to avoid sample charging. For the device structures shown in Fig. 1(a), the α-NPD film thickness of 100 nm was used. Finally, to complete the cathodes of the hole-only devices, about 10 nm of molybdenum oxide, MoO_x ($2 < x < 3$) (Mitsuwa Chemical), and 100 nm of aluminum (Nilaco) have been deposited onto the organic films. The deposition rates were 1 Å/s, 0.5 Å/s and 5 Å/s, for α-NPD, molybdenum oxide and Al, respectively.

The UPS experiments have been performed in a home-built, ultra-high vacuum set-up (base-pressure < 4×10^{-10} mbar) [14]. He I ($h\nu$ = 21.218 eV) UPS spectra have been acquired as a function of the polar emission angle θ using a SCIENTA SES-100 hemispherical analyzer, and integrated within ± 5°. The total instrumental energy resolution has been set to 50 meV. In the set-up employed here, the angle between the directions of the incoming photons and the emitted photoelectrons is fixed at 45°. Spectra are shown with respect to the Fermi level, E_F, of the spectrometer. The work function, ϕ, has been determined from the analysis of the secondary electron cut-offs, the sample being biased at –5 V. The current density-voltage (*J*–*V*) characteristics of the devices were obtained using a computer-controlled Keithley 2400 sourcemeter, using the ITO electrode as anode and the Al electrode as cathode. Molecular energy levels have been calculated by a density-functional theory (DFT) method in which an unrestricted open-shell wave function (B3LYP/6-31G**) and Becke's three-parameter exchange with the Lee, Young and Parr

correlation function (B3LYP) was used. In order to account for solid state effects and to match the experimental spectrum, these energies have then been rigidly shifted and broadened.

3. Results and discussion

3.1. As-prepared and rubbed α-6T films on ITO

Figure 1b shows the current density *J* as a function of the applied voltage *V* of the hole-only devices, either with as-deposited or with rubbed α–6T films. As discussed previously [13], the current densities *J* of the devices made with rubbed α–6T films are more than one order of magnitude higher than that for those made with as-deposited α–6T films. It is therefore important to understand how the charge injection barriers between ITO and the α–6T film, on one hand, and at the organic/organic interface, on the other, are affected by the change of orientation of the α–6T molecules caused by the mechanical rubbing.

This information is best obtained by UPS and work function measurements that can provide a full picture of the alignment of occupied energy levels with respect to E_F. In Fig. 2a are shown UPS spectra of an as-deposited α-6T film, taken at selected θ. As expected for a thickness of 15 nm, all valence band features are attributed to α-6T molecular states. In line with previously reported spectra [15,16], the peaks at lowest binding energies, centered at 1.07±0.01 eV and 1.80±0.01 eV, denoted "H" and "H-1", are related to the highest occupied molecular orbital (HOMO) and the HOMO-1 of the α-6T, respectively. Only minor spectral changes occur as a function of θ. Note that the photoelectron emission pattern from localized π-electronic states is strongly varying with the emission angle with respect to the normal of the molecular plane [17,18]. For relatively low photon energies $h\nu$ like the one used in the present experiments, the emission cone is, however, broadened, as compared to higher $h\nu$, with the maximum shifted to higher θ. Providing this intensity pattern for each molecule, the measured angular dependence

of the emission intensity is then consistent with the presence of α-6T domains of "standing " molecules that have a random in-plane orientation.

After rubbing of the film, notable changes in the overall spectral shape are observed, as shown in Fig. 2b. While some spectral features like **"**H" and "H-1" are reduced in intensity, others, like the shoulder at about 6 eV, are increased. This is consistent with the already observed [13] change of the average molecular orientation towards a "flat" configuration. Importantly, however, as shown in the inset of Fig. 2b, the binding energy of the "H" and "H-1" features does not change keeping the hole injection barrier from ITO to the α-6T films of 0.63 ± 0.01 eV constant. This is consistent with Fermi level alignment and indicates that the improved device performance following the rubbing procedure is not related to the charge injection at the α-6T/ITO interface.

The work function of the ITO substrate ϕ_{ITO} = 4.74 ± 0.03 eV is decreased by about $|\Delta_1|$ = 0.45 ± 0.01 eV upon adsorption of the α-6T molecular film. This decrease is partially reversed by about 0.16 ± 0.01 eV upon rubbing which translates into a increased ionization potential (IP) for the nominally "flat" α-6T films obtained by rubbing. The IPs as estimated from the sum of the workfunction and the onset of spectral weight at low binding energies are 4.92 ± 0.04 eV and 5.08 ± 0.04 eV, for the as-prepared, "standing" and rubbed, "flat" films, respectively. Note that the dependence of the IP on the molecular orientation is well understood and essentially caused by the modification of the surface dipole of the molecular film due to the change of the intramolecular bond orientation at the surface [19] and to a minor extent on the dependence of the polarization energy on the molecular packing [20].

3.2. Interface between α-6T and α-NPD films

In order to understand the electronic structures of the organic/organic interface and of the α-NPD films itself, in a next step, UPS was performed on 10-nm-thick α-NPD films on the already discussed as-deposited and rubbed α-6T substrates. The corresponding UPS spectra are shown in Figure 3a and 3b,

respectively. Spectral features are typical for α-NPD films which indicates that the α-6T films are completely covered [21,22]. As shown in the inset of Fig. 3b, at normal emission ($\theta = 0°$), the spectra of the two samples are almost identical but rigidly shifted to each other. Since the α-6T HOMO energy is unaffected by the rubbing, this shift of about $\delta_{HIB} = 0.24 \pm 0.02$ eV towards lower binding energy after rubbing is related to *a decrease of the hole injection barrier* at the organic/organic interface from 0.43 ± 0.01 eV to 0.19 ±0.01 eV which shall be considered to be one of the reasons for the higher current densities in the hole-only device structures. As illustrated in the diagrams displayed in Figures 4a and b, the type of energy level alignment at the α-NPD/α-6T interface observed here is typical for a vacuum level alignment regime at the organic/organic interface which is emphasized also by the only small and almost unchanged vacuum level offsets Δ_2 of 0.12 ± 0.02 eV and 0.08 ± 0.02 eV, for the samples with as-deposited and rubbed α-6T layers, respectively.

3.3. Molecular orientation in α-NPD films

At higher angles θ, the spectra of the α-NPD film prepared on the as-prepared, "standing" α-6T substrate (Fig. 3a) display only a minor angular dependence. This is consistent with the expected emission pattern from non-oriented molecules present in an amorphous film. The θ-dependence observed for the film deposited onto the rubbed α-6T substrate (Fig. 3b), on the other hand, is strikingly different. Here, the intensity of spectral features denoted "A", "B" and "C", at binding energies around 9 eV, 7 eV and 5 eV, changes significantly with θ. In particular, while feature "A" is decreased with increasing θ, "B" and "C" show a strong increase. This indicates that the photoelectron emission pattern is anisotropic and strongly dependent on the molecular orbitals involved. It must be concluded that α-NPD molecules or functional groups thereof are becoming oriented with respect to the substrate normal. While the flexible molecular structure of the α-NPD molecules prevents crystallization, a preferential orientation of α-NPD molecules is possible, as observed previously [4] for the thin film structure discussed over here. It is

obvious that these orientational changes are caused by the "flat" orientation of the α-6T molecules which serve as a growth template for the α-NPD film.

In order to obtain additional insight into the structural properties of the oriented α-NPD film, the molecular electronic structure has been calculated within the DFT framework. As shown in Fig. 5a, the splitting between the highest two occupied levels, denoted "H" and "H-1", is underestimated in the calculations, which indicates [23,24] that, in the films, the twist angle between the core of the molecule and the phenyl and naphtyl side groups is larger than for the optimized geometry of the free molecule. The spacing of all other ground state energy levels agrees well with UPS spectral features allowing an assignment of particular molecular orbital to experimental peaks. In particular, feature "B" is related to the molecular orbitals numbered "132", "133" and "134", which are almost exclusively localized on the α-NPD side groups (Fig. 5b). While feature "A" derives from the orbitals "108", "106" and "110" that have contributions at both the core of the molecule and the side groups. The opposite angular dependence of "A" and "B" is then another strong indication for a large twist between the center and the side groups while the molecules themselves are, in the average, oriented with respect to the normal of the substrate. Moreover, the increase of "B" with θ is consistent with a rather "flat" orientation of the phenyl and naphtyl side groups. Given this orientation, it may be conceived that the interaction of the side groups with the "flat" α-6T molecules at the interface may drive the overall molecular orientation of the α-NPD molecules that progresses into thicker films and to the surface region where it is observed by UPS. Note, that the spacing between "H" and "H-1" does not change between the two α-NPD films which indicates that the twist angle between the core of the molecule and the side groups is unchanged.

It may then also be conceived that a higher degree of order at the organic/organic interface may also improve the charge carrier transport. In particular, a "flat" and "face-to-face" orientation of the α-6T molecules and α-NPD phenyl side groups leads to *a larger spatial overlap of the π orbitals at the*

interface. Since the reduction of the total charge injection barrier from the ITO substrate to the α-NPD amounts only to 23 ± 1% of the barrier height, it must strongly be considered that the effective π-π overlap at the α-NPD/α-6T interface shall be another main reason for the the enhancement of the current densities after rubbing.

3.3. Energy level alignment at the organic-organic interface

The work function of the sample with the α-NPD film on top of the as-deposited α-6T film is ϕ = 4.41 ± 0.03 eV, slightly lower than that of ϕ = 4.54 ± 0.03 eV of the α-NPD film on the rubbed α-6T substrate. Because of the different orientation of the molecules, as expected, with 5.47 ± 0.04 eV and 5.36 ± 0.04 eV, the IPs of the two samples are also different from each other.

With all energy parameters at hand, the reason for the lowering of the charge injection barrier at the organic/organic interface and for the alignment of energy levels at the organic/organic interface may now be discussed. Here it is important to note that the shift of the α-NPD vacuum level with respect to that of the ITO substrate is about 0.33 ± 0.02 eV and 0.20 ± 0.02 eV, for the sample with the as-prepared and rubbed a-6T, respectively. The similarity of these two offsets indicate that the position of the α-NPD HOMO is determined by the equilibration of the electrochemical potential of the α-NPD films with that of the ITO substrate, as suggested for other organic/organic heterojunctions by Osikowicz *et al.* [25]. The values are quite similar because the electrochemical potential of an organic film is essentially that of the molecule itself. Given such an alignment, we propose that the change of the hole injection barrier hight δ_{HIB} is then given by the difference of the changes of the ionization potentials of the two organic films, on both sides of the heterojunction. Thus, $\delta_{HIB} \approx (IP_{\alpha\text{-}6T,1} - IP_{\alpha\text{-}6T,2}) - (IP_{\alpha\text{-}NPD,1} - IP_{\alpha\text{-}NPD,2}) = 0.27 \pm 0.06$ eV which is close to the measured change of the injection barrier of $\delta_{HIB} = 0.24 \pm 0.02$ eV. It is then clear that different to the case of Fermi level pinning [26], in the case of vacuum level alignment present in the device structure discussed over here, the energy of the HOMO-related hole transport level of α-NPD film

is *fundamentally determined by the surface dipoles of the molecular films* that relate to the intramolecular polar bond orientation at the interface.

4. Conclusions

Upon mechanical rubbing of an α-6T film prepared on an ITO substrate, subsequently deposited non-crystalline films of the α–NPD are found to become oriented. These orientational changes improve the performance of hole-only devices based on these α-NPD/α–6T heterojunctions and have been linked to changes of the energy level alignment and to the spatial overlap of the π orbitals of α-6T and of the α–NPD phenyl and naphthyl side groups at the organic/organic heterointerface. In the case of vacuum level alignment related to weak interactions at the organic/organic interface, the observed reduction of the hole injection barrier can be understood from changes in the intramolecular polar bond orientation at the surfaces of the two individual organic films. The results demonstrate that the charge injection efficiency across organic/organic heterointerfaces can be engineered by controlling the orientation-dependent surface dipoles and the π orbital orientation at the interface between the two organic films. Such a control can be achieved even for non-crystalline materials and simple *ex-situ* techniques.

Aknowlegdements

We acknowledge fruitful discussions with Yuanping Yi (School of Chemistry and Biochemistry and Center for Organic Photonics and Electronics, Georgia Institute of Technology, USA). This work has been supported by Grants-in-Aid for Scientific Research of Japan (No. 21760005, 20241034, and 20108012) and by the MARUBUN Foundation.

.

References

[1] C. W. Tang, S. A. Vanslyke, Appl. Phys. Lett. **51**, 913 (1987).

[2] Y. Shirota, H. Kageyama, Chem. Rev. **107**, 953 (2007).

[3] S. Chen, L. Deng, J. Xie, L. Peng, L. Xie, Q. Fan, W. Huang, Adv. Mater. **22**, 5227 (2010).

[4] D. Yokoyama, A. Sakaguchi, M. Suzuki, C. Adachi, Appl. Phys. Lett. **93**, 173302 (2008).

[5] R. A. Marcus, J. Chem. Phys. **24**, 966 (1956).

[6] H. Bässler, Phys. Status Solidi B **175**, 15 (1993).

[7] M. Era, T. Tsutsui, S. Saito, Appl. Phys. Lett. **67**, 2436 (1995).

[8] Y. Toda, H. Yanagi, Appl. Phys. Lett. **69**, 2315 (1996).

[9] H. Yanagi, S. Okamoto, Appl. Phys. Lett. **71**, 2563 (1997).

[10] I. Frischeisen, D. Yokoyama, A. Endo, C. Adachi, W. Brütting, Org. Electron. **12**, 809 (2011).

[11] D. Yokoyama, Y. Setoguchi, A. Sakaguchi, M. Suzuki, C. Adachi, Adv. Funct. Mater. **20**, 386 (2010).

[12] T. Arai, K. Goushi, H. Nomura, T. Edura, C. Adachi, Appl. Phys. Lett. **99**, 053303 (2011).

[13] T. Matsushima, H. Murata, Appl. Phys. Lett. **98**, 253307 (2011).

[14] F. Bussolotti, S. W. Han, Y. Honda, R. Friedlein, Phys. Rev. B **79**, 245410 (2009).

[15] C. E. Heiner, J. Dreyer, I. V. Herbel, N. Koch, H.-H. Titze, W. Widdra, B. Winter, Appl. Phys. Lett. **87**, 093601 (2005).

[16] M. Grobosch, M. Knupfer, Org. Electron. **9**, 767 (2008).

[17] R. Friedlein, X. Crispin, C. D. Simpson, M. D. Watson, F. Jäckel, W. Osikowicz, S. Marciniak, M. P. de Jong, P. Samorí, S. K. M. Jönsson, M. Fahlman, K. Müllen, J. P. Rabe, W. R. Salaneck, Phys. Rev. B **68**, 195414 (2003).

[18] S. Kera, S. Tanaka, H. Yamane, D. Yoshimura, K. K. Okudaira, K. Seki, N. Ueno, Chem. Phys. **325**,113 (2006).

[19] S. Duhm, G. Heimel, I. Salzmann, H. Glowatzki, R. Johnson, A. Vollmer,J. Rabe, N. Koch, Nature Mater. **7**, 326 (2008).

[20] R. Friedlein, X. Crispin, M. Pickholz, M. Keil, S. Stafström, W. R. Salaneck, Chem. Phys. Lett. **354**, 389 (2002).

[21] M. Kröger, S. Hamwi, J. Meyer, T. Riedl, W. Kowalsky, A. Kahn, Appl. Phys. Lett. **95**, 123301 (2009).

[22] K. Kanai, K. Koizumi, S. Ouchi, Y. Tsukamoto, K. Sakanoue, Y. Ouchi, K. Seki, Org. Electron. **11**, 188 (2010).

[23] N. Koch, G. Heimel, J. Wu, E. Zojer, R. L. Johnson, J.-L. Brédas, K. Müllen, J. P. Rabe, Chem. Phys. Lett. **390**, 413 (2005).

[24] R. Friedlein, F. von Kieseritzky, S. Braun, C. Linde, W. Osikowicz, J. Hellberg, W. R. Salaneck, Chem. Commun. **2005**, 1974 (2005).

[25] W. Osikowicz, M. P. de Jong, W. R. Salaneck, Adv. Mater. **10**, 4213 (2007).

[26] W. Chen, S. Chen, H. Huang, D. C. Qi, X. Yu. Gao, A. T. S. Wee, Appl. Phys. Lett. **92**, 063308 (2008).

Figure Captions

Fig. 1. (a) Chemical structures of the α-6T and α-NPD molecules, (b) the device structure of the hole-only devices composed of ITO, α-6T, α-NPD, molybdenum oxide and Al, and (c) the *J-V* characteristics of the hole-only devices with as-deposited and rubbed α–6T layers.

Fig. 2. UPS spectra of the (a) as-deposited and (b) rubbed α-6T films as a function of the polar photoelectron emission angle θ. (c) Low-binding-energy region of the normal-emission spectra of as-deposited and rubbed films.

Fig. 3. UPS spectra of the α-NPD films prepared on top of (a) as-deposited and (b) rubbed α-6T films as a function of the polar photoelectron emission angle θ. (c) Low-binding-energy region of the normal-emission spectra of the α-NPD films prepared on as-deposited and rubbed α-6T films.

Fig. 4. Scheme of the energy levels of hole-only devices: (a) α-NPD/as-deposited α-6T/ITO and (b) α-NPD/rubbed α-6T/ITO.

Fig. 5. (a) UPS spectrum of the α-NPD film (on rubbed α-6T), (b) a simulated spectrum derived from (c) calculated molecular orbital energies, shown at the bottom of the graph. Wave functions of selected α-NPD molecular orbitals are related to peaks in the simulated spectrum.

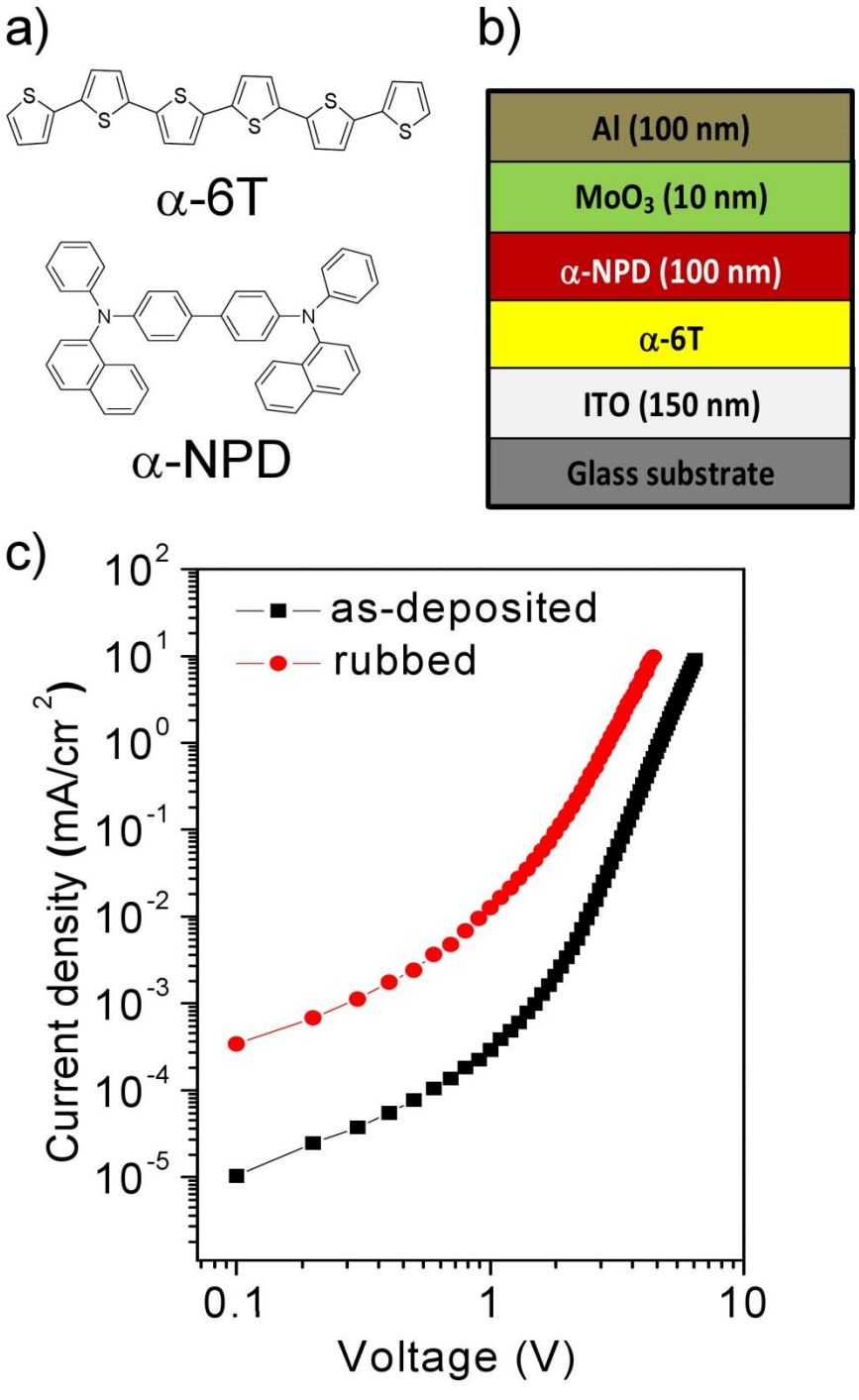
a)
α-6T
α-NPD
b)
Al (100 nm)
MoO3 (10 nm)
α-NPD (100 nm)
α-6T
ITO (150 nm)
Glass substrate
c)
as-deposited
rubbed
Current density (mA/cm2)
Voltage (V)
0.1
1
10

Figure 1

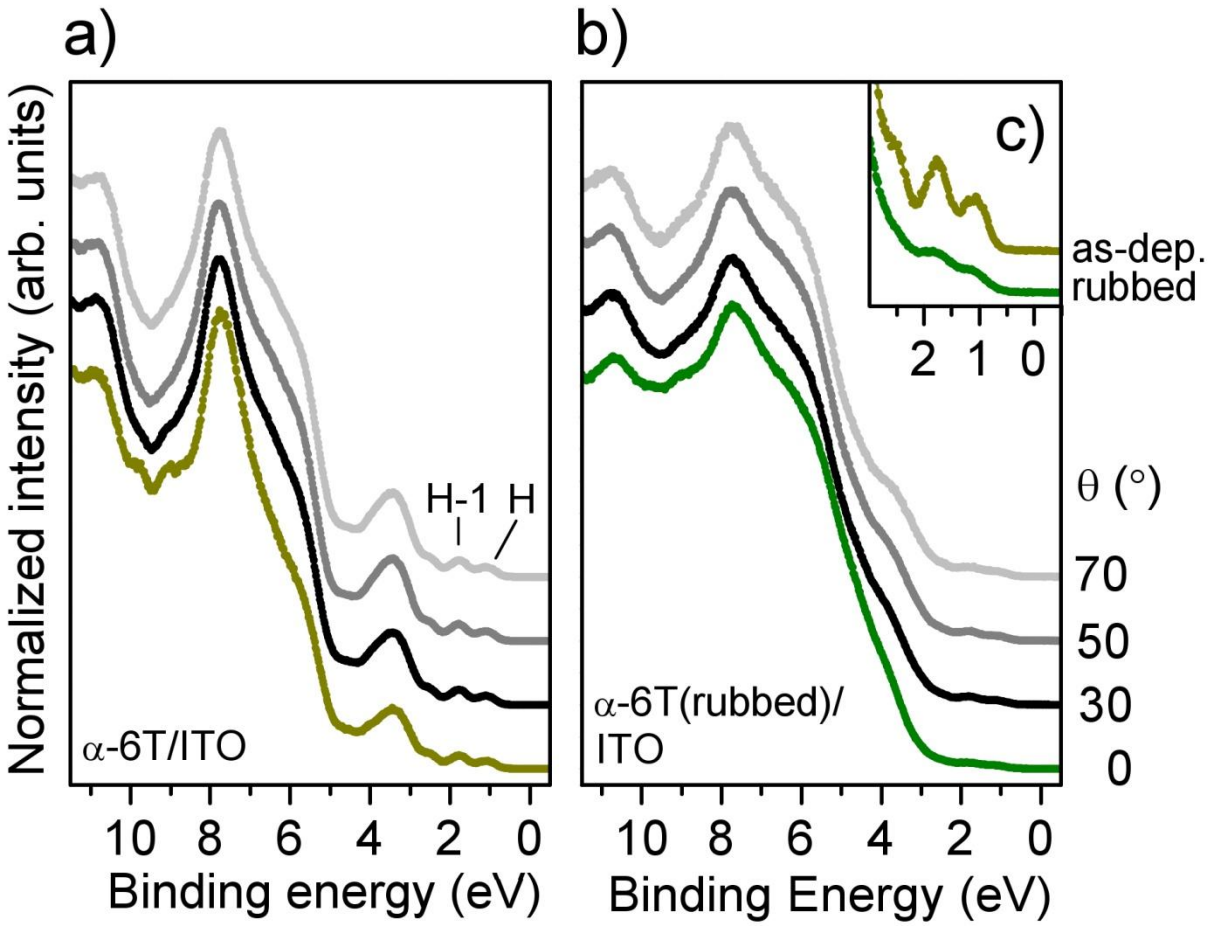
a)
b)
c)
Normalized intensity (arb. units)
H-1
H
α-6T/ITO
10 8 6 4 2 0
Binding energy (eV)
α-6T(rubbed)/
ITO
10 8 6 4 2 0
Binding Energy (eV)
2 1 0
as-dep.
rubbed
θ (°)
70
50
30
0

Figure 2

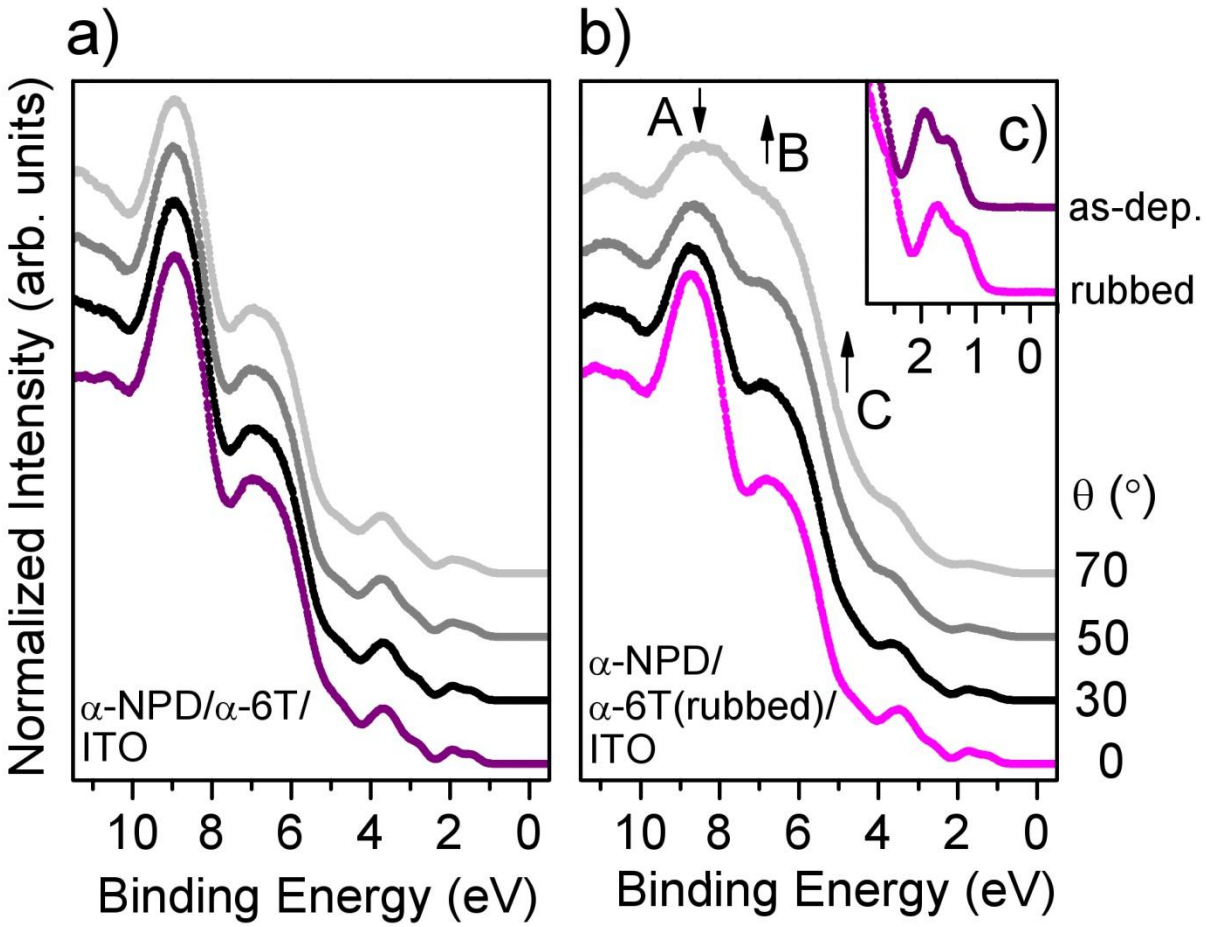
a)
b)
c)
Normalized Intensity (arb. units)
α-NPD/α-6T/
ITO
α-NPD/
α-6T(rubbed)/
ITO
A
B
C
as-dep.
rubbed
θ (°)
70
50
30
0
10 8 6 4 2 0
Binding Energy (eV)
2 1 0

Figure 3

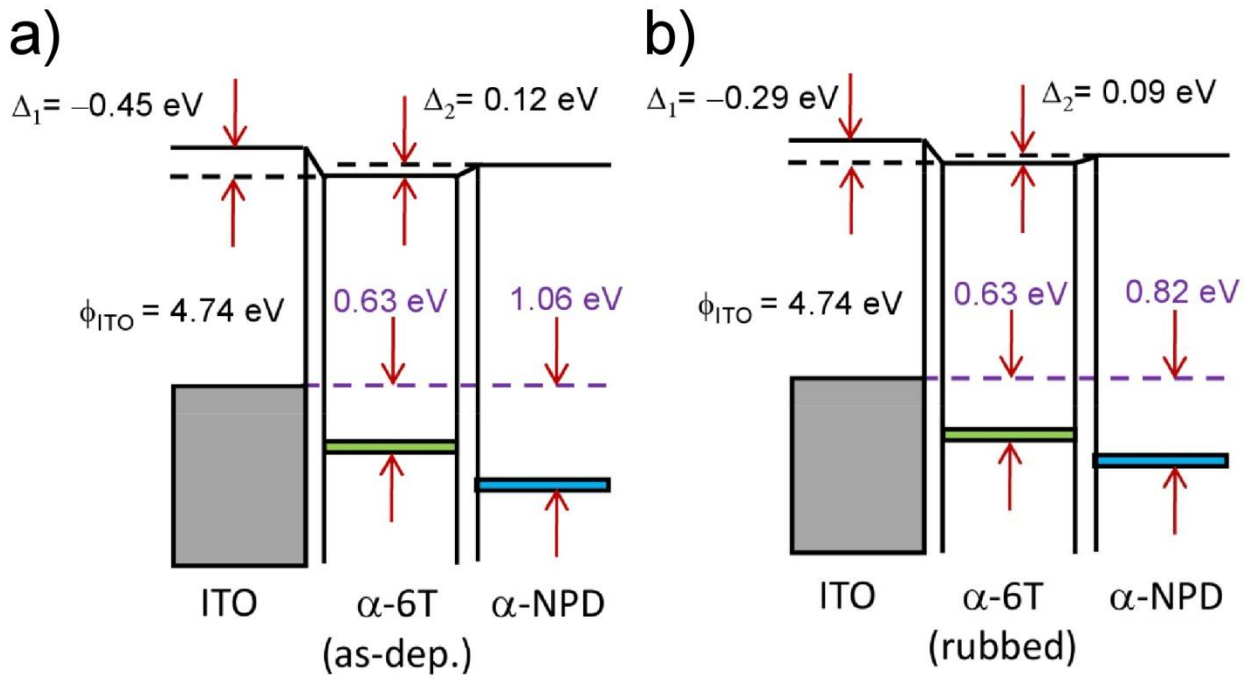
a)
Δ1= –0.45 eV
Δ2= 0.12 eV
ϕITO = 4.74 eV
0.63 eV
1.06 eV
ITO
α-6T
(as-dep.)
α-NPD
b)
Δ1= –0.29 eV
Δ2= 0.09 eV
ϕITO = 4.74 eV
0.63 eV
0.82 eV
ITO
α-6T
(rubbed)
α-NPD

Figure 4

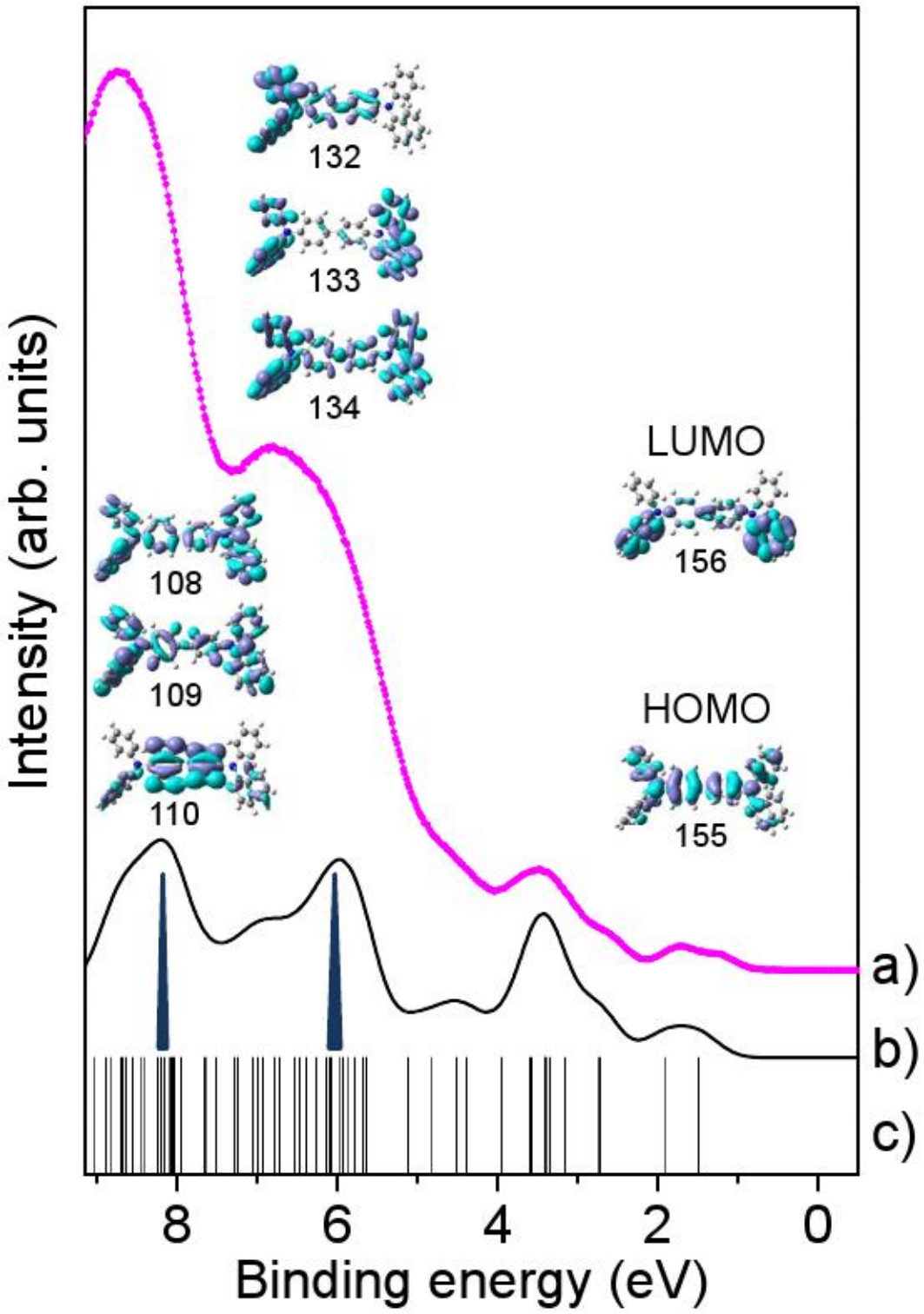
Intensity (arb. units)
132
133
134
LUMO
156
108
109
110
HOMO
155
a)
b)
c)
8
6
4
2
0
Binding energy (eV)

Figure 5